Table 5. Expression data of significant increased or decreased spot volumes in HeLa cells treated with pyrrolizilactone.[a]

Spot no.	Pyrrolizilactone	MG-132	Proteasome inhibitor II	Lactacystin	Geldanamycin	Radicicol	Uniprot AC	Protein name
662	0.71**	0.84**	0.82**	0.75**	0.74**	0.74**	P21399	cytoplasmic aconitate hydratase
1563	1.14**	1.22**	1.33**	1.09	0.93	0.96	O00487	26S proteasome non-ATPase regulatory subunit 14
2064	0.63**	0.94	1.02	0.94	0.91*	0.79**	O00571	ATP-dependent RNA helicase DDX3X
975	0.61**	0.94	0.59**	0.59**	0.99	0.94	O75083	WD repeat protein 1
1399	0.73**	0.79**	0.81**	0.67**	0.74**	0.88**	P04075	Fructose-bisphosphate aldolase A
1754	5.29**	2.65**	2.53**	2.76**	1.64**	1.30**	P04792	heat-shock protein β-1
1757	7.29**	3.34**	3.64**	4.80**	2.08**	1.96**	P04792	heat-shock protein β-1
934	9.24**	4.85**	5.18**	5.52**	6.17**	6.91**	P08107	heat shock 70 kDa protein 1A/1B
949	6.31**	5.51**	4.98**	5.51**	7.68**	8.13**	P08107	heat shock 70 kDa protein 1A/1B
1975	5.22**	5.06**	4.28**	5.99**	6.52**	7.27**	P08107	heat shock 70 kDa protein 1A/1B
902	1.52**	1.18*	1.39**	1.25	1.17	1.03	P20700	lamin-B1
1731	0.85**	0.78**	0.86**	0.79**	0.74**	0.80**	P25788	proteasome subunit α type 3
1744	0.81**	0.88**	0.95	0.82**	1.08*	0.91**	P30040	endoplasmic reticulum protein ERp29
1000	0.88**	0.77**	1.01	0.80**	0.83**	0.95	P31939	bifunctional purine biosynthesis protein PURH
1011	0.74**	0.78**	0.90*	0.81**	0.91*	0.90*	P31948	stress-induced-phosphoprotein 1
1499	0.56**	0.87**	0.77**	0.80**	0.70**	1.12*	P52895	aldo-keto reductase family 1 member C2
1137	0.53**	0.65**	0.85**	0.57**	0.68**	0.72**	Q01518	adenylyl cyclase-associated protein 1
1142	0.63	0.91	0.99	0.81**	0.67**	0.65**	Q01518	adenylyl cyclase-associated protein 1
1174	0.76	0.76**	0.83**	0.61**	0.76**	0.84**	Q16658	fascin
1438	1.44	1.15**	1.18**	1.27**	1.22**	1.06	Q9BQ04	RNA-binding protein 4B

[a] The mean ratio between control and each compound was calculated. Non-repeated-measures ANOVA and Dunnett's test for post hoc analysis were performed. Asterisks indicate significant differences from respective controls (* $p < 0.05$, ** $p < 0.01$).

has a different site of action than that of these two compounds. Consistent with the inhibitory activity of pyrrolizilactone against the proteasome, an accumulation of ubiquitylated proteins was observed in HeLa cells treated with 30 μM pyrrolizilactone (Figure 4B). Furthermore, flow cytometric analysis demonstrated that both pyrrolizilactone and MG-132 induced cell-cycle arrest at G1 and G2/M in HeLa cells (Figure 4C). These data indicate that pyrrolizilactone inhibits proteasome activity both in cell-free and cell-based systems.

Discussion

Various profiling approaches for target identification by using comprehensive datasets (incorporating large quantities of phenotypic data related to genetic and chemical perturbations) have been reported and successfully used to identify and validate specific molecular targets of bioactive small molecules.[6] As these indirect approaches employ profile comparison of a test compound to a reference dataset, we can easily and rapidly speculate as to the mode of action without the requirement for large quantities of the test compound (and any chemical modification). However, this methodology often suffers from the disadvantage of ambiguity in the prediction and characterization of compounds that do not show any distinct phenotype in the profiling system. In this regard, a multifaceted approach that uses several distinct profiling systems holds promise for elucidating the mode of action of an agent, with greater speed and reliability.

In this study, we identified the molecular target of pyrrolizilactone, a novel cytotoxic fungal metabolite, by using two phenotypic profiling systems: MorphoBase and ChemProteoBase. Although each technique alone could have suggested that the proteasome was the plausible target for pyrrolizilactone, the probability of such a prediction is not sufficiently great. In MorphoBase profiling, the PCA scores of pyrrolizilactone were projected around the proteasome-inhibitor cloud, consisting of relatively low probability scores ($Score_{proteasome} = 1.71$). In ChemProteoBase profiling, pyrrolizilactone was found to overlap clusters of proteasome and HSP90 inhibitors, without any clear discrimination between these. Cross-validation of these two profiling methods provided a clear indication of which plausible targets should be validated first; therefore, we began by testing a 26S proteasome as the target for pyrrolizilactone.

The 20S catalytic core particle (CP) of 26S proteasome was identified as a molecular target of the natural product lactacystin.[13] Additionally, various proteasome inhibitors have been found: 1) to cause cell cycle arrest; 2) to exhibit unique cytotoxicity patterns against the NCI60 panel of 60 cell-lines in vitro;[14] and 3) to exert antitumor activity in vivo. Based on these observations, the proteasome represents an effective therapeutic target for cancer treatment.[15] Following the demonstration of dramatic clinical efficacy for the boronate bortezomib against multiple myeloma, many structurally diverse proteasome inhibitors targeting the CP (both natural and synthetic) have been developed.[16] The eukaryotic CP consists of three active β-subunits, β1, β2, and β5, which are responsible for the caspase-like, trypsin-like, and chymotrypsin-like proteolytic activities of the proteasome, respectively. The role of these active sites was addressed by site-directed mutagenesis of the yeast orthologue: inactivation of β5 by a mutation in their catalytic threonine resulted in significant cell-growth defect and accumulation of proteasome substrates;[17] mutations in β1 or β2 sites had less impact on phenotype. Thus, the chymotrypsin-like sites have long been considered the only

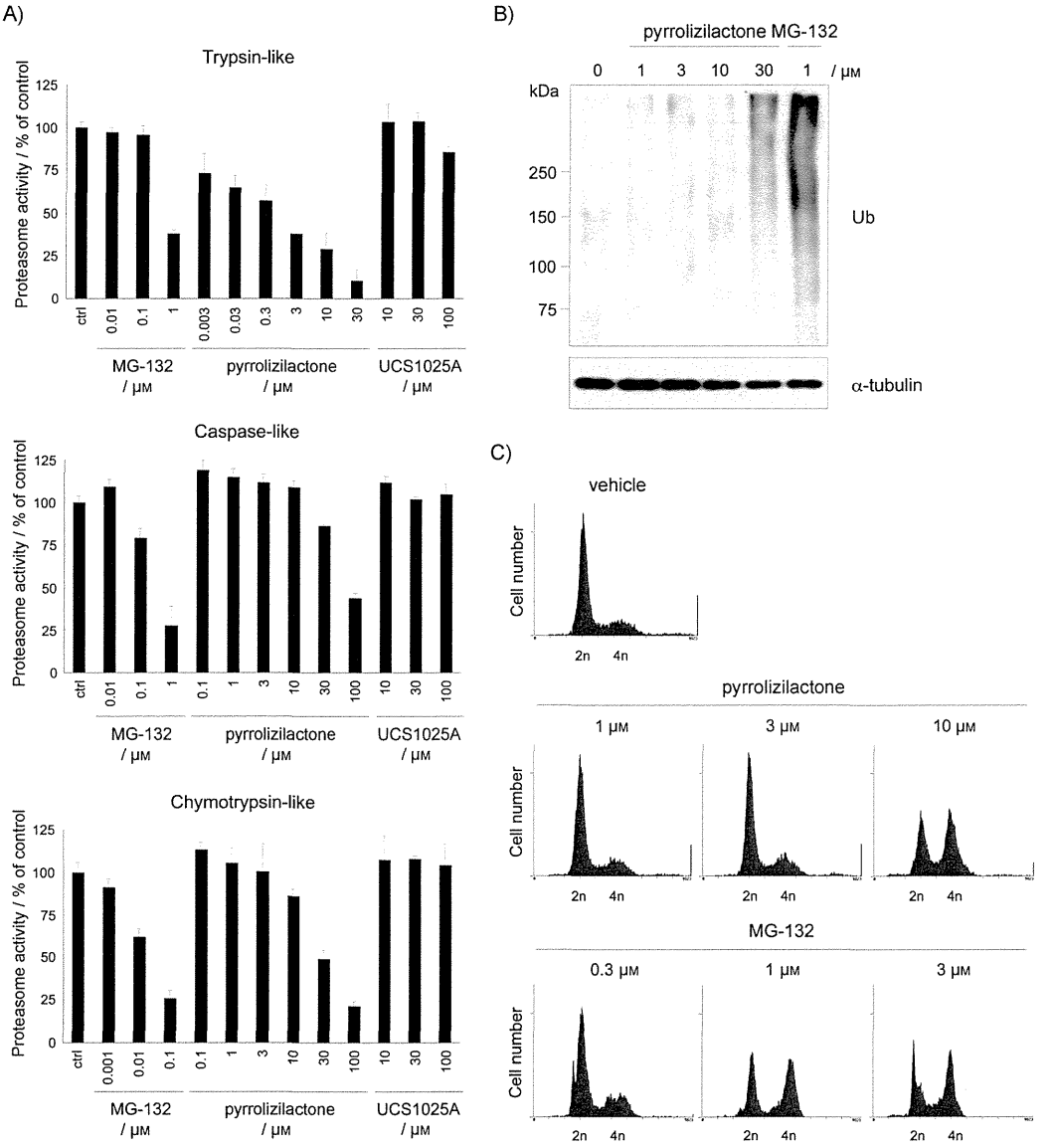

Figure 4. Pyrrolizilactone inhibits proteasome activity. A) In vitro effect of pyrrolizilactone, MG-132, and UCS1025A on chymotrypsin-like, trypsin-like, and caspase-like activities of human 20S proteasome. B) Effect of pyrrolizilactone and MG-132 on accumulation of ubiquitylated protein in HeLa cells. HeLa cells were treated with compounds for 20 h. Cell lysates were subject to immunoblotting with antibodies against the indicated targets. C) Cell cycle progression of HeLa cells was monitored by DNA content analysis by using flow cytometry after 24 h incubation with the indicated compounds. 2n = diploid state, 4n = tetraploid state.

Table 6. IC_{50} values [μM] of pyrrolizilactone, MG-132, and UCS1025A for proteasomal activity.

Compound	Trypsin-like	Chymotrypsin-like	Caspase-like
pyrrolizilactone	1.6	29	84
MG-132	0.8	0.02	0.4
UCS1025A	>100	>100	>100

suitable anticancer targets, and drug development has focused most extensively on specific inhibitors of this site. However, Kisselev and colleagues recently reported that the cytotoxicity of proteasome inhibitors in most multiple myeloma cell-lines does not correlate with inhibition of the chymotrypsin-like sites, but rather with loss of site-specificity and with inhibition of the trypsin-like sites.[18] Shortly thereafter, they developed cell-permeable peptide epoxyketones specific for the trypsin-like proteasome site, and demonstrated the compounds' sensitizing effects on multiple myeloma cells to conventional boronate proteasome inhibitors, such as bortezomib and carfilzomib.[19] In this study, we demonstrated that pyrrolizilactone inhibits specifically trypsin-like sites. Although growth defects and accumulation of ubiquitylated proteins did not seem to be as dramatic as for MG-132 (Figure 4), it was well consistent with the phenotype induced by β2 inactivation. Because coinhibition of trypsin- and caspase-like sites is now expected for the next generation of proteasome inhibitors, the potentiating effects of pyrrolizilactone on cytotoxicity mediated by chymotorypsin-like inhibitors and the detailed mechanism of action are currently under investigation.

To date, only peptide epoxyketones (above) have been reported to be cell-permeable β2-site-specific inhibitors, whereas the natural product inhibitors identified so far (e.g., β-lactones lactacystin[13] and marizomib/salinosporamide A,[20] tripeptides epoxomicin[21] and tyropeptins,[22] and the cyclopeptide TMC-95A)[23] selectively inhibit chymotrypsin-like sites. Our newly identified proteasome inhibitor, pyrrolizilactone, has a structure that is distinct from others: a tricyclic skeleton composed of a pyrrolizidinone fused to γ-lactone that connects to a decalin moiety, and a unique molecular target, the β2-component of the proteasome. Thus, pyrrolizilactone is an example of a natural nonpeptide inhibitor with novel distinct chemical and biological properties.

The only fungal metabolites structurally related to pyrrolizilactone are the two antitumor antibiotics CJ-16264[24] and UCS1025A.[9] Nakai and colleagues demonstrated that UCS1025A shows a selective growth defect in telomere-shortened yeast and directly inhibits human telomerase with an IC_{50} of 1.3 μM in a cell-free assay.[10] In this study, we investigated whether the structurally related UCS1025A also inhibits proteasome activity. UCS1025A was not positioned in the proteasome inhibitor cluster by MorphoBase profiling systems (Figure 2), and it did not inhibit proteolytic activity of the 20S proteasome at up to 100 μM (Figure 4A). The chemical structural properties differ between pyrrolizilactone and UCS1025A in the substitution pattern of the methyl group and the relative configuration of a decalin unit: pyrrolizilactone possesses a *cis* configuration in the decalin unit with five substituted methyl groups, whereas UCS1025A possesses a *trans* configuration with one methyl group. The differences in biological activity between the two pyrrolizidinones are assumed to be related to the stereochemistry of their respective decalin fragments. The pyrrolizilactone structure appears to yield a novel mode of interaction with proteasome; therefore, studies on the biosynthesis and chemistry have been initiated to establish the structure–activity relationship and to develop more potent trypsin-like proteasome inhibitors.

Conclusions

To identify the molecular target of pyrrolizilactone, we applied two phenotypic profiling systems—MorphoBase and ChemProteoBase. These profiling methodologies rapidly gave us an insight into the mode of action of pyrrolizilactone, and we were able to establish that pyrrolizilactone is a unique 26S proteasome inhibitor. Unlike conventional proteasome inhibitors, which attack chymotrypsin-like sites, pyrrolizilactone inhibits the trypsin-like proteolytic activity of the proteasome. Thus, it might be not only an effective adjuvant for current treatment of multiple myeloma, but also a useful chemical tool for further study on the role of the proteasome. This study clearly demonstrates the effectiveness of our microbial metabolite fraction library and phenotypic profiling systems for natural products drug discovery. Follow-up studies on these screening platforms should provide improvements for the prompt discovery of novel anticancer natural products with unique mechanism of action.

Experimental Section

Materials: Pyrrolizilactone was isolated from the fermentation broth of the fungal strain RKB3564,[5] previously identified as an epoxyquinol-producing strain.[25] UCS1025A was kindly provided by Kyowa Hakko Kirin (Shizuoka, Japan). All other inhibitors were obtained from the RIKEN Natural Products Depository (NPDepo, Wako, Japan).

Cell culture and cell proliferation assay: *src*^{ts}-NRK cells,[26] the rat kidney cells infected with ts25, a T-class mutant of Rous sarcoma virus Prague strain (a gift from Dr. Yoshimasa Uehara, Iwate Medical University School of Pharmacy), were cultured at a permissive temperature (32 °C) in MEM (Sigma–Aldrich), supplemented with 10% calf serum (PAA Laboratories). HeLa cells were cultured in DMEM (Invitrogen/Life Technologies), supplemented with 10% fetal bovine serum (FBS; Sigma–Aldrich). The human promyelocytic leukemia cell-line HL-60[27] (RIKEN Cell Bank, Wako, Japan) was cultured in RPMI 1640 (Invitrogen), supplemented with 10% FBS. tsFT210 cells,[28] the mouse temperature-sensitive cdc2 mutant cell-line of the mammary carcinoma FM3A (a gift from Dr. Fumio Hanaoka, Gakushuin University), was cultured in RPMI 1640 supplemented with 5% CS. Cell proliferation was determined by using a Cell Count Reagent SF (No. 07553-15, Nacalai Tesque, Kyoto, Japan) according to the manufacturer's instructions. Briefly, following 48 h exposure, a $^1/_{10}$ volume of WST-8 solution was added to each well, and the plates were incubated for 1 h. Absorbance (450 nm) was analyzed with a microplate reader and expressed as percentage relative to vehicle-treated cells.

Target estimation by MorphoBase profiling: MorphoBase profiling was performed as previously described.[7] Briefly, *src*^{ts}-NRK and HeLa cells were plated on poly-D-lysine-coated, black, 96-well μClear-base plates (Greiner Bio-one). After exposure to a test compound, the cells were fixed with 3.7% formalin and stained with Hoechst 33342 (Sigma–Aldrich). Bright-field images and nuclear images were acquired on an IN Cell Analyzer 2000 (GE Healthcare). Approximately 1000 cells from these images were analyzed with custom-designed image analysis algorithms to partition individual cells and to measure 12 user-defined descriptors, such as nuclear and cellular area, for each cell. To characterize phenotypic responses at the well level, the average, median, and standard deviation of each parametric measurement were calculated. A total of 71 parameters were normalized to the average of corresponding control values of DMSO-treated cells. Common logarithmic outputs were then applied to the subsequent statistical analysis. For PCA, the eigenvalue/eigenvector of the covariance matrix was calculated, and the resulting principal component scores were displayed in a 2D scatter plot. The prediction of a target molecule or the mechanism of action of a test drug was demonstrated by performing two statistical computations: probability scores and the ranking of the nearest neighbors, to a test compound determined by Euclidean distance between selected compound and reference compounds.

Target estimation by ChemProteoBase profiling: ChemProteoBase profiling was performed as previously described.[8] Briefly, HeLa cells were treated with the specified concentration of pyrrolizilactone for 18 h. Proteome analysis of cell lysate was performed by using 2D difference gel electrophoresis (2D DIGE) system (GE Healthcare), and images of the gels were analyzed by Progenesis SameSpots (Nonlinear Dynamics, Newcastle upon Tyne, UK). Of more than 1000 spots detectable in each 2D gel, 296 variational spots were found to be in common between gels of reference compound-treated cells, and were selected as described.[29] Next, the volume of each spot was normalized by using the average of

the corresponding control values from DMSO-treated HeLa cells. From the normalized volumes of the 296 spots, cosine similarity between compounds was calculated, and hierarchical clustering analysis was performed in Cluster 3.0 (clustering method; centroid linkage with the means of uncentered correlation).[30] The predictive dendrogram was visualized with Java Treeview 1.1.3.[31]

20S proteasome activity assay: In vitro proteasome activity assays were performed as previously described[21] with purified human erythrocyte-derived 20S proteasome (Boston Biochem, Cambridge, MA). Proteasomal chymotrypsin-like, trypsin-like, and caspase-like activities were measured by using the fluorogenic substrates suc-LLVY-AMC, z-ARR-AMC, and z-LLE-AMC, respectively (Calbiochem/Merck Millipore). The test compound was preincubated with enzyme at 30 °C for 30 min, and the reaction was then initiated by substrates addition. After 1 h incubation at 30 °C, AMC product formation was measured with a spectrofluorometer (λ_{ex} = 355 nm, λ_{em} = 460 nm).

Flow cytometry: Flow cytometry was performed as previously described.[8] Briefly, ethanol-fixed cells were washed with PBS and stained in propidium iodide (PI) buffer (PBS; 137 mM NaCl, 2.7 mM KCl, 10 mM Na_2HPO_4, 1.76 mM KH_2PO_4, pH 7.4, containing 50 μg mL^{-1} PI and 2 μg mL^{-1} RNase A; Nacalai Tesque) for 30 min. DNA content was analyzed with a Cytomics FC500 cytometer (Beckman Coulter).

Immunoblotting: Immunoblotting was performed as described previously[8] with anti-ubiquitin (Santa Cruz Biotechnology, Santa Cruz, CA) and anti-α-tubulin (Sigma–Aldrich) antibodies.

Acknowledgements

We thank Dr. Ryuichiro Nakai (Kyowa Hakko Kirin) for kindly providing UCS1025A. We also thank Hisae Kondo, Kazue Noda, and Akiko Okano for their technical assistance, and Dr. Konstanty Wierzba for a critical review of the manuscript. This work was supported in part by Grant-in-Aid for Scientific Research (KAKENHI), Health and Labour Sciences Research Grant, and the Program for Promotion of Basic and Applied Researches for Innovations in Bio-oriented Industry.

Keywords: cancer · ChemProteoBase · MorphoBase · natural products · pyrrolizilactone

[1] D. J. Newman, G. M. Cragg, *J. Nat. Prod.* **2012**, *75*, 311–335.
[2] a) H. Osada, *Biosci. Biotechnol. Biochem.* **2010**, *74*, 1135–1140; b) T. S. Bugni, M. K. Harper, M. W. B. McCulloch, J. Reppart, C. M. Ireland, *Molecules* **2008**, *13*, 1372–1383; c) Y. Tu, B. Yan, *Methods Mol. Biol.* **2012**, *918*, 117–126; d) C. J. Schulze, W. M. Bray, M. H. Woerhmann, J. Stuart, R. S. Lokey, R. G. Linington, *Chem. Biol.* **2013**, *20*, 285–295.
[3] a) N. Kato, S. Takahashi, T. Nogawa, T. Saito, H. Osada, *Curr. Opin. Chem. Biol.* **2012**, *16*, 101–108; b) H. Osada, T. Nogawa, *Pure Appl. Chem.* **2012**, *84*, 1407–1420.
[4] a) T. Nogawa, A. Okano, S. Takahashi, M. Uramoto, H. Konno, T. Saito, H. Osada, *Org. Lett.* **2010**, *12*, 4564–4567; b) T. Nogawa, S. Takahashi, A. Okano, M. Kawatani, M. Uramoto, T. Saito, H. Osada, *J. Antibiot.* **2012**, *65*, 123–128; c) S. Panthee, S. Takahashi, H. Takagi, T. Nogawa, E. Oowada, M. Uramoto, H. Osada, *J. Antibiot.* **2011**, *64*, 509–513.
[5] T. Nogawa, M. Kawatani, M. Uramoto, A. Okano, H. Aono, Y. Futamura, H. Koshino, S. Takahashi, H. Osada, *J. Antibiot.* **2013**; DOI: 10.1038/ja.2013.55.
[6] a) C. P. Hart, *Drug Discovery Today* **2005**, *10*, 513–519; b) E. Tashiro, M. Imoto, *Bioorg. Med. Chem.* **2012**, *20*, 1910–1921; c) Y. Futamura, M. Muroi, H. Osada, *Mol. BioSyst.* **2013**, *9*, 897–914; d) S. Ziegler, V. Pries, C. Hedberg, H. Waldmann, *Angew. Chem.* **2013**, *125*, 2808–2859; *Angew. Chem. Int. Ed.* **2013**, *52*, 2744–2792.
[7] Y. Futamura, M. Kawatani, S. Kazami, K. Tanaka, M. Muroi, T. Shimizu, K. Tomita, N. Watanabe, H. Osada, *Chem. Biol.* **2012**, *19*, 1620–1630.
[8] M. Muroi, S. Kazami, K. Noda, H. Kondo, H. Takayama, M. Kawatani, T. Usui, H. Osada, *Chem. Biol.* **2010**, *17*, 460–470.
[9] a) R. Nakai, H. Ogawa, A. Asai, K. Ando, T. Agatsuma, S. Matsumiya, S. Akinaga, Y. Yamashita, T. Mizukami, *J. Antibiot.* **2000**, *53*, 294–296; b) T. Agatsuma, T. Akama, S. Nara, S. Matsumiya, R. Nakai, H. Ogawa, S. Otaki, S. Ikeda, Y. Saitoh, Y. Kanda, *Org. Lett.* **2002**, *4*, 4387–4390.
[10] R. Nakai, H. Ishida, A. Asai, H. Ogawa, Y. Yamamoto, H. Kawasaki, S. Akinaga, T. Mizukami, Y. Yamashita, *Chem. Biol.* **2006**, *13*, 183–190.
[11] a) Y. Kawazoe, A. Nakai, M. Tanabe, K. Nagata, *Eur. J. Biochem.* **1998**, *255*, 356–362; b) A. Maloney, P. A. Clarke, S. Naaby-Hansen, R. Stein, J.-O. Koopman, A. Akpan, A. Yang, M. Zvelebil, R. Cramer, L. Stimson, W. Aherne, U. Banerji, I. Judson, S. Sharp, M. Powers, E. deBilly, J. Salmons, M. Walton, A. Burlingame, M. Waterfield, P. Workman, *Cancer Res.* **2007**, *67*, 3239–3253.
[12] J. Adams, M. Behnke, S. Chen, A. A. Cruickshank, L. R. Dick, L. Grenier, J. M. Klunder, Y.-T. Ma, L. Plamondon, R. L. Stein, *Bioorg. Med. Chem. Lett.* **1998**, *8*, 333–338.
[13] G. Fenteany, R. F. Standaert, W. S. Lane, S. Choi, E. J. Corey, S. L. Schreiber, *Science* **1995**, *268*, 726–731.
[14] J. Adams, V. J. Palombella, E. A. Sausville, J. Johnson, A. Destree, D. D. Lazarus, J. Maas, C. S. Pien, S. Prakash, P. J. Elliott, *Cancer Res.* **1999**, *59*, 2615–2622.
[15] a) J. B. Almond, G. M. Cohen, *Leukemia* **2002**, *16*, 433–443; b) S. Frankland-Searby, S. R. Bhaumik, *Biochim. Biophys. Acta Rev. Cancer* **2012**, *1825*, 64–76.
[16] a) C. S. Arendt, M. Hochstrasser, *Proc. Natl. Acad. Sci. USA* **1997**, *94*, 7156–7161; b) P. Chen, M. Hochsrasser, *Cell* **1996**, *86*, 961–972; c) W. Heinemeyer, M. Fischer, T. Krimmer, U. Stachon, D. H. Wolf, *J. Biol. Chem.* **1997**, *272*, 25200–25209.
[17] A. F. Kisselev, W. A. van der Linden, H. S. Overkleeft, *Chem. Biol.* **2012**, *19*, 99–115.
[18] M. Britton, M. M. Lucas, S. L. Downey, M. Screen, A. A. Pletnev, M. Verdoes, R. A. Tokhunts, O. Amir, A. L. Goddard, P. M. Pelphrey, D. L. Wright, H. S. Overkleeft, A. F. Kisselev, *Chem. Biol.* **2009**, *16*, 1278–1289.
[19] A. C. Mirabella, A. A. Pletnev, S. L. Downey, B. I. Florea, T. B. Shabaneh, M. Britton, M. Verdoes, D. V. Filippov, H. S. Overkleeft, A. F. Kisselev, *Chem. Biol.* **2011**, *18*, 608–618.
[20] R. H. Feling, G. O. Buchanan, T. J. Mincer, C. A. Kauffman, P. R. Jensen, W. Fenical, *Angew. Chem.* **2003**, *115*, 369–371; *Angew. Chem. Int. Ed.* **2003**, *42*, 355–357.
[21] L. Meng, R. Mohan, B. H. B. Kwok, M. Elofsson, N. Sin, C. M. Crews, *Proc. Natl. Acad. Sci. USA* **1999**, *96*, 10403–10408.
[22] I. Momose, R. Sekizawa, H. Hashizume, N. Kinoshita, Y. Homma, M. Hamada, H. Iinuma, T. Takeuchi, *J. Antibiot.* **2001**, *54*, 997–1003.
[23] Y. Koguchi, J. Kohno, M. Nishio, K. Takahashi, T. Okuda, T. Ohnuki, S. Komatsubara, *J. Antibiot.* **2000**, *53*, 105–109.
[24] Y. Sugie, H. Hirai, H. Kachi-Tonai, Y.-J. Kim, Y. Kojima, Y. Shiomi, A. Sugiura, Y. Suzuki, N. Yoshikawa, L. Brennan, J. Duignan, L. H. Huang, J. Sutcliffe, N. Kojima, *J. Antibiot.* **2001**, *54*, 917–925.
[25] H. Kakeya, R. Onose, H. Koshino, A. Yoshida, K. Kobayashi, S. Kageyama, H. Osada, *J. Am. Chem. Soc.* **2002**, *124*, 3496–3497.
[26] H. Osada, H. Koshino, K. Isono, H. Takahashi, G. Kawanishi, *J. Antibiot.* **1991**, *44*, 259–261.
[27] H. Osada, J. Magae, C. Watanabe, K. Isono, *J. Antibiot.* **1988**, *41*, 925–931.
[28] H. Osada, C.-B. Cui, R. Onose, F. Hanaoka, *Bioorg. Med. Chem.* **1997**, *5*, 193–203.
[29] M. Kawatani, H. Takayama, M. Muroi, S. Kimura, T. Maekawa, H. Osada, *Chem. Biol.* **2011**, *18*, 743–751..
[30] M. J. L. de Hoon, S. Imoto, J. Nolan, S. Miyano, *Bioinformatics* **2004**, *20*, 1453–1454.
[31] A. J. Saldanha, *Bioinformatics* **2004**, *20*, 3246–3248.

Received: August 2, 2013
Published online on October 25, 2013

The Journal of Antibiotics (2014), 1–7

www.nature.com/ja

ORIGINAL ARTICLE

RK-1355A and B, novel quinomycin derivatives isolated from a microbial metabolites fraction library based on NPPlot screening

Chung Liang Lim[1,2], Toshihiko Nogawa[3], Masakazu Uramoto[1], Akiko Okano[3], Yayoi Hongo[4], Takemichi Nakamura[4], Hiroyuki Koshino[4], Shunji Takahashi[1,3], Darah Ibrahim[2] and Hiroyuki Osada[1,3]

Two novel quinomycin derivatives, RK-1355A (1) and B (2), and one known quinomycin derivative, UK-63,598 (3), were isolated from a microbial metabolites fraction library of *Streptomyces* sp. RK88-1355 based on Natural Products Plot screening. The structural elucidation of 1 and 2 was established through two-dimensional NMR and mass spectrometric measurements. They belong to a class of quinomycin antibiotics family having 3-hydroxyquinaldic acid and a sulfoxide moiety. They are the first examples for natural products as a quinoline type quinomycin having a sulfoxide on the intramolecular cross-linkage. They showed potent antiproliferative activities against various cancer cell lines and they were also found to exhibit moderate antibacterial activity.
The Journal of Antibiotics advance online publication, 5 February 2014; doi:10.1038/ja.2013.144

Keywords: antimicrobial activities; fraction library; microbial metabolites; quinomycin; spectral database; *streptomyces* sp.; structure elucidation

INTRODUCTION

Natural products and their derivatives are major sources in the discovery of novel drug candidates.[1] Natural products displayed a unique and vast chemical diversity, and also diversity in biological activities, making natural products libraries favorable and attractive in drug discovery.[2] In recent years, natural products-based drug discovery is gaining attention, which implies that natural products serve an evolving role in future drug discovery.[3] Microorganisms were known to possess immense capacity to produce various bioactive secondary metabolites[4] with diverse potential activities. Hence, microbial metabolites have been a significant source of pharmaceutical leads and therapeutic agents.[5,6] They are of great interest for human to isolate them and develop as novel drug candidates. These metabolites are also utilized as potential bioprobes[7] in chemical biology studies, mainly as a tool for investigation of biological functions.[8] To date, many secondary metabolites have been reported. Nevertheless, not all of them have been isolated nor have their latent useful activities examined due to their wide range of physicochemical properties and relatively low abundance. Thus, we have attempted to construct a microbial metabolites fraction library by a systematic separation method and develop a spectral database, namely NPPlot (Natural Products Plot), based on photodiode array (PDA) detector-attached LC/MS analysis.[9] On the basis of NPPlot comparison method, structurally unique metabolites could be identified efficiently and rapidly. Also, the efforts for identifying known compounds would be reduced significantly. As previously reported, our methodology of constructing a fraction library led us to identify and isolate several novel compounds, including verticilactam[10] from *Streptomyces spiroverticillatus* JC-8444, a tautomycin producer,[11–13] spirotoamides A and B[14] from *Streptomyces griseochromogenes* JC82-1223, a tautomycetin producer,[15,16] novel furaquinocins I and J[17] and 6-dimethylalylindole-3-carbaldehyde[18] from *Streptomyces reveromyceticus* SN-593, a reveromycin producer.[19] These findings have revealed the advantages of utilizing fraction libraries for the isolation and probing of the activities of natural products.

The microbial metabolites fraction library was prepared following the scheme as described in the previous paper.[9] To take advantage of a fraction library and to facilitate the distinction of novel metabolites from known compounds rapidly, we have developed a unique spectral database, namely NPPlot, based on PDA-LC/MS analysis to obtain the UV absorption and mass spectra of each metabolite within each fraction in the fraction library. These information were important for us to discriminate known compounds and to discover structurally novel metabolites. The open spectral database was unable to distinguish metabolite groups between microbial strains as compared with NPPlot, thus making it a useful tool for the discovery of novel metabolites.

[1]Antibiotics Laboratory, RIKEN, Saitama, Japan; [2]Industrial Biotechnology Research Laboratory, School of Biological Sciences, Universiti Sains Malaysia, Penang, Malaysia; [3]RIKEN Center for Sustainable Research Science, Saitama, Japan and [4]RIKEN Global Research Cluster, Saitama, Japan
Correspondence: Dr H Osada, Antibiotics Laboratory, RIKEN, 2-1 Hirosawa, Wako, Saitama 351-0198, Japan.
E-mail: hisyo@riken.jp
Received 31 October 2013; revised 3 December 2013; accepted 12 December 2013

NPPlot is a distribution map of metabolites plotted on a two-dimensional (2D) area by retention time of HPLC on *x* axis and *m/z* values on *y* axis. On the basis of NPPlot screening, we could discover novel compounds and also search for specific metabolites group for each microbial strain through the comparison of distribution patterns generated from several microbial strains. On the basis of this novel method, we have generated NPPlot from five different microbial strains and compared their distribution patterns. A group of compounds showing a characteristic distribution in the region of molecular mass around 1150 and retention time around 25 min was detected in strain RK88-1355 (Figure 1). On screening for structurally unique secondary metabolites using the NPPlot comparison method, we identified two unknown peaks and one known peak with identical UV absorption pattern, but slightly different mass spectra in fractions of *Streptomyces* sp. RK88-1355. The related fractions were purified by a C_{18}-HPLC to afford compounds **1** (8.8 mg) and **2** (1.5 mg), together with one known compound **3** (5.7 mg), respectively (Table 1). We report herein the structures and biological activities of these compounds, designated RK-1355A (**1**) and B (**2**), as shown in Figure 2.

RESULTS AND DISCUSSION

We have isolated novel quinomycin derivatives, RK-1355A (**1**) and B (**2**) from *Streptomyces* sp. RK88-1355, which was isolated from a soil sample collected in Tohoku area, Japan in 1988. This strain was deposited in RIKEN NPDepo (Natural Products Depository). The molecular formula of compound **1** was established to be $C_{53}H_{62}N_{10}O_{15}S_2$ by HRESIMS (found: *m/z* 1143.3923 $[M+H]^+$, calcd for $C_{53}H_{63}N_{10}O_{15}S_2$ 1143.3916), which required the addition of an oxygen atom to **3** (UK-63,598).[20] The UV absorption spectrum showed λ_{max} (MeOH) values at 218, 230, 298 and 356 nm (Table 1), suggesting the presence of 3-hydroxyquinaldic acid.[20–23] On the basis of interpretation of IR spectrum, the presence of hydroxyl group (3370 cm^{-1}), an ester group (1735 cm^{-1}) and an amide group (1655 and 1520 cm^{-1}) were confirmed by the appearance of corresponding bands in the spectrum. These observations were characteristic of a depsipeptide with an aromatic 3-hydroxyquinaldic acid chromophore. The C–H stretching absorptions were observed at 2920 cm^{-1} and 2850 cm^{-1}, respectively. There was an additional IR band observed at 1014 cm^{-1}, implying the presence of a sulfoxide in **1**.[24] The ^1H NMR spectrum in chloroform-*d* suggested that **1** contained nine methyl groups. It also contained six exchangeable protons at δ 11.29 (OH) and δ 8.85 (NH) with 2H integral values, respectively, and at δ 6.49 (NH) and δ 6.40 (NH) based on integration values and HSQC interpretation. These exchangeable protons were confirmed by the addition of D_2O in the ^1H NMR spectrum. Two of the exchangeable protons were observed as a single sharp signal at δ 11.29 with 2H integral value, suggesting that **1** had two hydroxyl groups, which were overlapped in ^1H NMR spectrum. At δ 8.85 (br d, $J=9.2$ Hz), two exchangeable protons were observed with 2H integral value, which confirmed the presence of two secondary amides that were overlapped. The ^{13}C NMR spectrum of **1** showed 51 signals, which did not match with the molecular formula obtained from HR-MS/MS.

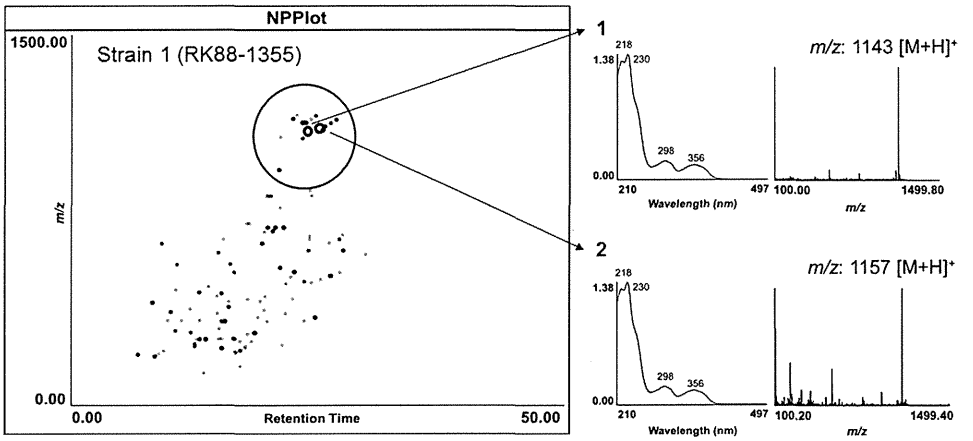

Figure 1 NPPlot for *Streptomyces* sp. strain RK88-1355 showing the characteristic distribution of metabolites (highlighted region) plotted by retention time of HPLC on *x* axis and *m/z* values on *y* axis. Light color spot on NPPlot indicates one single metabolite and dark color spot implies an overlapped spot containing more than one or few metabolites, which are closely related. A full color version of this figure is available at *The Journal of Antibiotics* journal online.

Table 1 Physicochemical properties of compounds 1 and 2

	Compound 1	*Compound 2*
Appearance	Pale yellow amorphous solid	Pale yellow amorphous solid
Optical rotation	$[\alpha]_{589}^{24}$ −83.8° (*c* 0.04, MeOH)	$[\alpha]_{589}^{24}$ −76.2° (*c* 0.04, MeOH)
Molecular formula	$C_{53}H_{62}N_{10}O_{15}S_2$	$C_{54}H_{64}N_{10}O_{15}S_2$
UV (MeOH) λ_{max} (log ε) nm	218 (4.72), 230 (4.73), 298 (3.89), 356 (3.79)	218 (4.79), 230 (4.79), 298 (3.96), 356 (3.87)
IR ν_{max} (ATR) cm^{-1}	3370, 2920, 2850, 1735, 1655, 1520, 1014	3380, 2920, 1735, 1655, 1510, 1014
ESIMS (*m/z*)	1143 $[M+H]^+$	1157 $[M+H]^+$
HRESIMS (*m/z*)		
Found	1143.3923 $[M+H]^+$	1157.4089 $[M+H]^+$
Calculated	1143.3916 for $C_{53}H_{63}N_{10}O_{15}S_2$	1157.4072 for $C_{54}H_{65}N_{10}O_{15}S_2$

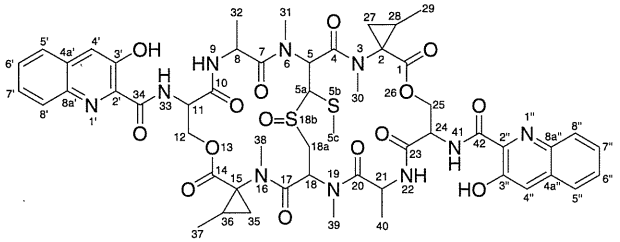

1

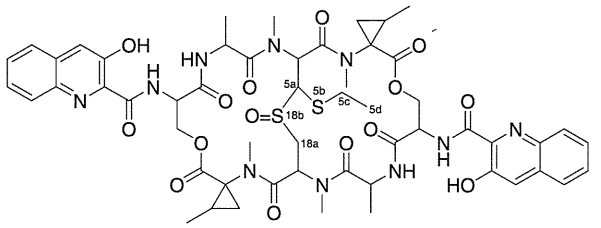

2

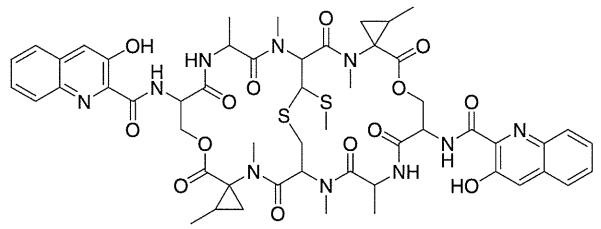

3 (UK-63,598)

Figure 2 Structures of compounds **1**, **2** and **3**, UK-63,598.

On the basis of detailed interpretation of ^{13}C DEPT, HSQC and HMBC spectra, one methyl signal at δ 11.8 and one quaternary signal at δ 153.7 were found, each of which was observed as a signal with strong intensity, respectively, were overlapped completely. These observations led to the identification of 53 carbon signals, which were attributed to 9 methyls, 5 methylenes, 19 methines that bore 10 olefinic carbons and 20 quaternary carbons, including 10 carbonyls. These assignments were verified by the ^{13}C DEPT experiment and HSQC spectral data (Table 2).

The planar structure of **1** was determined by 2D NMR analysis, as shown in Figures 3, 4 and 5. The connections between protons and carbons were established by HSQC spectrum. The structure of quinomycin with quinoline moiety for **1** was constructed based on interpretation of DQF-COSY, HSQC and HMBC spectra and confirmed by MS/MS spectrum. The COSY and HMBC spectra showed the presence of four partial structures as shown in Figure 3. The partial structure A, 3-hydroxyquinaldic acid moiety was implied by the presence of nine sp^2 carbons (C-2′ to C-8a′) and five related aromatic protons (δ 7.47, δ 7.48, δ 7.67, δ 7.68, δ 7.69) with a proton of hydroxyl group (δ 11.29) and the COSY correlations of H-5′ to H-6′, H-6′ to H-7′ and H-7′ to H-8′. This aromatic moiety was confirmed by the following HMBC correlations: from H-7′ to C-8a′, from H-6′ to C-4a′, from H-5′ to C-8a′, from H-8′ to C-4a′, from H-4′ to C-4a′, C-5′, C-3′, C-8a′ and C-2′, and from OH-3′ to C-2′, C-3′ and C-4′. The COSY spectrum of partial structure B showed a methyl–methine–methylene spin system and it was determined as a 2-methyl-1-methylaminocyclopropanecarboxylic acid moiety through the long-range couplings from H_2-27, H-29 and H-30 to C-2 and from H_2-27 to

Table 2 ^{13}C NMR chemical shifts for compounds 1 and 2 in $CDCl_3$

	1	*2*		*1*	*2*
Position	δ_C	δ_C	*Position*	δ_C	δ_C
1	169.1	169.1	33-NH		
2	47.1	47.1	34	168.6	167.5
4	169.2	169.4	35	26.0	26.1
5	54.7	54.8	36	25.1	25.0
5a	71.3	68.9	37	11.8[a]	11.8[a]
5c	18.7	28.7	38	36.4	36.0
5d		17.0[a]	39	30.0	30.0
7	173.6	174.0	40	17.0	14.7
8	45.9	45.8	41-NH		
9-NH			42	168.6	169.3
10	167.6	167.6	2′	133.6	133.6
11	50.7	51.0	3′	153.7[a]	153.8[a]
12	64.1	64.3	4′	121.3	121.3
14	169.3	168.6	4a′	132.4	132.4
15	47.2	47.2	5′	126.8	126.8
17	169.7	169.6	6′	129.0	129.0
18	50.5	50.5	7′	127.7	127.7[a]
18a	50.0	50.2	8′	128.5	128.5
20	172.8	172.9	8a′	141.2	141.2
21	46.0	45.9	3′-OH		
22-NH			2″	133.7	133.7
23	167.6	168.6	3″	153.7[a]	153.8[a]
24	51.0	50.7	4″	121.4	121.4
25	64.3	64.1	4a″	132.4	132.5
27	26.3	26.3	5″	126.9	126.9
28	25.0	25.2	6″	129.0	129.0
29	11.8[a]	11.8[a]	7″	127.7	127.7[a]
30	35.9	36.4	8”	128.5	128.6
31	31.4	31.3	8a″	141.2	141.2
32	16.8	17.0[a]	3″-OH		

^{13}C NMR at 125 MHz was referenced to $CDCl_3$ (δ 77.0).
[a]These signals were observed as overlapping signals.

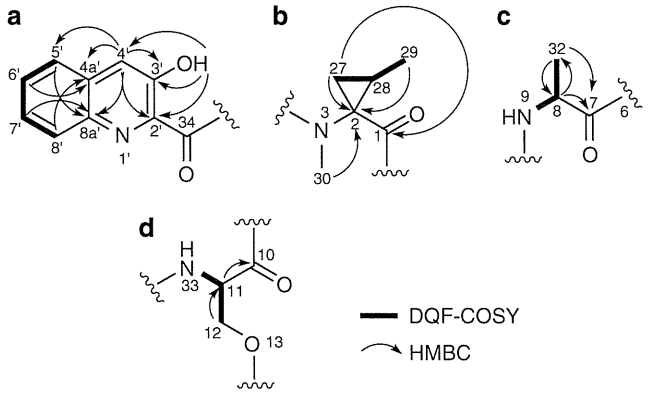

Figure 3 Partial structures of compound **1**.

C-1. The partial structure C was indicated to be an alanine residue by the COSY correlations of H-8 with NH-9 and H-32 to H-8, and confirmed by the HMBC correlations from H-8 to C-7 and C-32, from H-32 to C-7 and C-8. The COSY correlations from H-11 to NH-33 and H-12, and the HMBC correlations from H-11 to C-10 and H-12 to C-11 confirmed the partial structure D as a serine residue. The COSY and HMBC correlations revealed the presence of two alanine

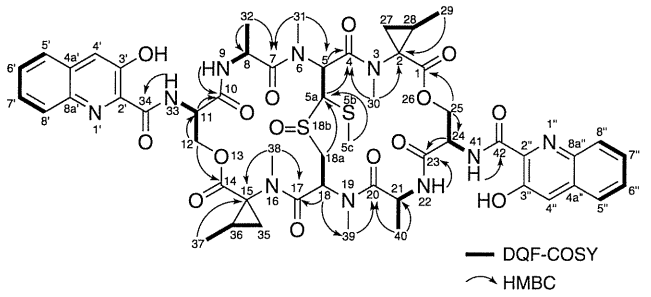

Figure 4 Selected DQF-COSY (bold lines) and HMBC correlations (solid arrows) observed for **1**.

residues (Ala and Ala′), two serine residues (Ser and Ser′), two 2-methyl-1-methylaminocyclopropanecarboxylic acid moieties and two 3-hydroxyquinaldic acid chromophores in compound **1**. The HMBC correlations from H-12 to C-14 and from H-25 to C-1 confirmed the ester linkages between the serine residues and the 2-methyl-1-methylaminocyclopropanecarboxylic acid moieties. The connections of the alanyl–serinyl residues were revealed by the long-range correlations from NH-9 to C-10 and from NH-22 to C-23, respectively. The attachments of the aromatic 3-hydroxyquinaldic acid chromophore moieties to the serine residues were clearly indicated by the long-range correlations from NH-33 and NH-41 to C-34 and C-42 of the carbonyl carbons for the chromophore units. Furthermore, the

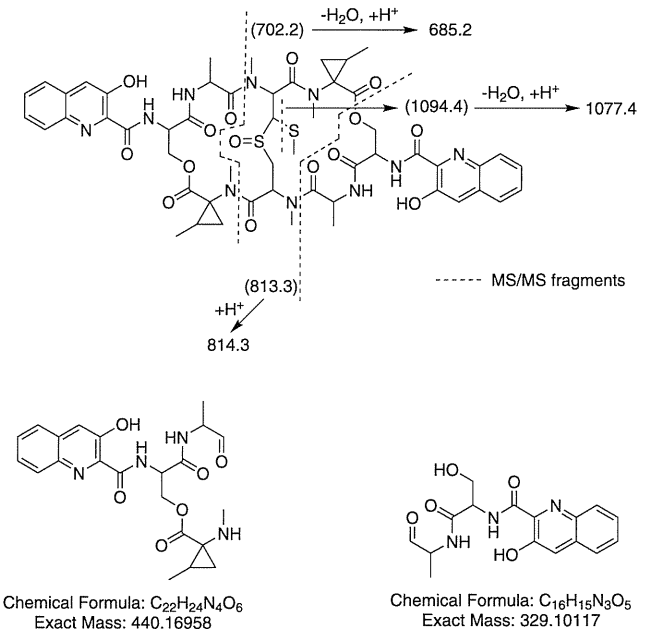

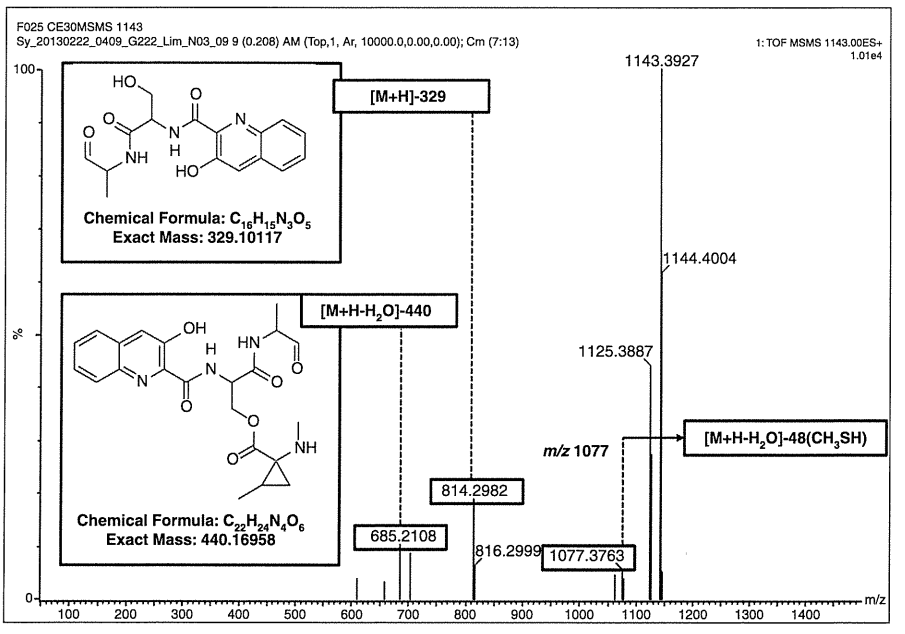

Figure 5 MS/MS fragments pattern (dotted lines) and MS/MS spectrum observed for **1**.

connectivities of these partial structures were established through the long-range correlations from H-30 to C-4, from NH-9 to C-10, from H_2-12 to C-14, from H-38 to C-17, and from NH-22 to C-23. For the connection of sulfur-containing intramolecular cross-linkage, which resembled cysteine sulfoxide moiety, it was determined by the COSY correlations of H-5 to H-5a and H-18 to H-18a, and the HMBC correlations from H-18 to C-39 and C-17, from H-5a and H-5 to C-4, from H-31 to C-5 and C-7, and from H-5c and H-18a to C-5a. This connection was confirmed by the ^{13}C NMR chemical shifts of C-5a (71.3 p.p.m.), C-18a (50.0 p.p.m.) and C-5c (18.7 p.p.m.) (Figure 4). Owing to the acquisition of an additional oxygen atom in **1**, HR-MS/MS analysis was conducted to confirm the site of oxidation. The fragmentation showing a loss of S-methyl (*m/z* 1077 $[M+H]^+$) from the parent compound was observed, indicating that the oxidation in **1** was resided at the Cys′ sulfur atom. Thus, the existence of a sulfoxide moiety in **1** was confirmed, which was supported by the IR band at 1014 cm^{-1} described previously. The cyclic depsipeptide skeleton of **1** was confirmed by HR-MS/MS analysis, in which a small fragment ion peak was observed on *m/z* value of 1077 $[M+H-H_2O-CH_3SH]^+$, indicating the dehydration and loss of fragment S-methyl from the protonated compound, which confirmed the presence of S-methyl group in **1** (Figure 5). A fragment ion peak also appeared on *m/z* value of 685 $[M+H-H_2O-C_{22}H_{24}N_4O_6]^+$, which indicates the dehydration and elimination of fragment $C_{22}H_{24}N_4O_6$ from the protonated compound **1**. Another fragment ion peak was observed on *m/z* value of 814 $[M+H-C_{16}H_{15}N_3O_5]^+$, implying the elimination of fragment $C_{16}H_{15}N_3O_5$ from the protonated compound **1**. These fragmentation patterns give rise to the skeleton of quinomycin with 3-hydroxyquinaldic acid chromophore. On the basis of the above NMR and MS spectroscopic analyses, the structure of **1** was determined as shown in Figure 2.

The compound **2** had the molecular formula of $C_{54}H_{64}N_{10}O_{15}S_2$ based on HRESIMS interpretation (found: *m/z* 1157.4089 $[M+H]^+$, calcd for $C_{54}H_{65}N_{10}O_{15}S_2$ 1157.4072), in which its molecular mass is 14 units higher than that of **1**. The UV spectrum of **2** showed the characteristic absorptions at 218, 230, 298 and 356 nm (Table 1), suggesting the presence of a 3-hydroxyquinaldic acid chromophore,[20–23] which was identical to that of **1**. The IR spectrum also indicated the presence of hydroxyl group (3380 cm^{-1}), an ester group (1735 cm^{-1}) and an amide group (1655 and 1510 cm^{-1}) as observed in compound **1**. The C–H stretching absorption was observed at 2920 cm^{-1} in the IR spectrum. A sulfoxide moiety was revealed by the presence of an IR band at 1014 cm^{-1}, identical to that of **1**.[24] The similarities between compounds **1** and **2** suggested that **2** was an analog of **1**. Compound **2** was analogous to **1** with S-ethyl derivative at C-5a. It was revealed by MS/MS spectra, which showed a fragment ion peak at *m/z* of 1093 $[M-H-EtSH]^-$, indicating the elimination of fragment S-ethyl from the deprotonated compound, thus confirmed the existence of S-ethyl group. Similar to compound **1**, HR-MS/MS experiment for **2** was carried out to determine the site of oxidation due to its additional oxygen atom. The observation of S-ethyl fragment lost (*m/z* 1093 $[M-H]^-$) indicated that the oxidation for the parent compound was resided at the Cys′ sulfur atom, thus revealing a sulfoxide moiety in **2**. The ^1H NMR spectrum was very similar to that of **1**, except for the disappearance of a singlet methyl signal instead of the observation of a new triplet methyl signal at 1.37 p.p.m. ($J=7.4$ Hz). The ^{13}C NMR spectrum was nearly identical with that of **1**, except for slight differences in chemical shifts of carbon signals around 18–28 p.p.m. The ^{13}C DEPT experiment and HSQC spectral data revealed that **2** has an extra methylene signal implying the replacement of ethyl derivative at C-5a in **2** instead of methyl group in **1**. Therefore, compound **2** was analogous to **1** with S-ethyl derivative at C-5a as shown in Figure 2. For compound **2**, the presence of two alanine residues (Ala and Ala′), two serine residues (Ser and Ser′), two 2-methyl-1-methylaminocyclopropanecarboxylic acid moieties and two 3-hydroxyquinaldic acid chromophores were revealed by the COSY and HMBC spectra. The connection of intramolecular cross-linkage (cysteine sulfoxide moiety) was established by the COSY correlations of H-5 to H-5a and H-18 to H-18a, and the HMBC correlations from H-18a to C-5a, from H-5c to C-5a and from H-5d to C-5c, and was supported by the ^{13}C NMR chemical shifts of C-5a (68.9 p.p.m.), C-18a (50.2 p.p.m.), C-5c (28.7 p.p.m.) and C-5d (17.0 p.p.m.). Thus, the structure of **2** was determined as shown in Figure 2 based on NMR and MS spectroscopic analyses.

Compounds **1–3** were subjected to several bioassays *in vitro*. Their cytotoxicities against various cancer cell lines, which included HL-60, HeLa, tsFT210 and *src*^{ts}-NRK were evaluated. Also, their antibacterial activities against *Staphylococcus aureus* 209 (a gram-positive bacteria), and *Escherichia coli* HO141 (a gram-negative bacteria), and antifungal activities against *Candida albicans* JCM1542, *Aspergillus fumigatus* Af293 and *Magnaporthe oryzae* kita-1 were tested. All tested compounds showed potent antiproliferative activities against various cancer cell lines at the submicromolar range of their IC_{50} values (Table 3). They also displayed moderate bactericidal activities, but have relatively little effects against fungi (Table 4).

In this research, we have constructed a microbial metabolites fraction library and a novel type of spectral database named NPPlot based on PDA-LC/MS analysis, which is a 2D data plotted by physicochemical properties of metabolites for screening of novel compounds efficiently. On the basis of this screening method, we have discovered and isolated two novel quinomycin derivatives, **1** and **2**, which contain a characteristic 3-hydroxyquinaldic acid chromophore and sulfoxide moiety. Their structures were determined by NMR and MS/MS analyses. Both compounds differ only on the sulfur-containing intramolecular cross-linkage, with **1** having S-methyl group and **2** having S-ethyl derivative. Although there have been several semi synthetic and natural products literatures reported the Cys and Cys′ sulfoxide analogs of echinomycin (quinomycin),[25,26] **1** and **2** are the first natural products as a quinoline type quinomycin having a

Table 3 ***In vitro*** **cytotoxicities (IC_{50}: μg ml^{-1}) of compounds 1–3**

	Mammalian cancer cell lines			
Compounds	*HeLa*	*HL-60*	*tsFT210*	*src*^{ts}*-NRK*
1	0.16	0.15	0.56	1.2
2	0.043	0.045	0.36	0.94
3	0.00021	0.00043	0.0071	0.029

Table 4 Antimicrobial activities (IC_{50}: μg ml^{-1}) of compounds 1–3

	Gram-positive	*Gram-negative*	*Fungi*		
Compounds	*S. aureus*	*E. coli*	*A. fumigatus*	*M. oryzae*	*C. albicans*
1	0.48	1.4	>10	3.1	>10
2	0.35	1	>10	3.6	>10
3	0.017	0.066	>10	0.82	8.7

Abbreviations: *S. aureus*, *Staphylococcus aureus* 209; *E. coli*, *Escherichia coli* HO141; *A. fumigatus*, *Aspergillus fumigatus* Af293; *M. oryzae*, *Magnaporthe oryzae* kita-1 and *C. albicans*, *Candida albicans* JCM1542.

sulfoxide moiety. These compounds showed potent antiproliferative activities against various cancer cell lines and exhibited moderate antibacterial activity. Thus, these results demonstrated the advantages of fraction library and NPPlot for the discovery of novel metabolites efficiently and rapidly.

EXPERIMENTAL PROCEDURE

General experimental procedures

All solvents and reagents were of analytical grade and were purchased from commercial sources. UV spectra and optical rotations were recorded on a BECKMAN DU 530 Life Science UV/Vis spectrophotometer (Brea, CA, USA) and a HORIBA SEPA-300 high sensitive polarimeter (HORIBA, Kyoto, Japan), respectively. IR spectra were recorded on a HORIBA FT-720 IR spectrometer with a DuraSampl IR II ATR instrument. NMR spectra were recorded on a JEOL ECA-500 FT-NMR spectrometer at 500 MHz for ^{1}H NMR and 125 MHz for ^{13}C NMR. Chemical shifts were reported in p.p.m. and referenced against the residual undeuterated solvent. Mass spectra were obtained on an AB Sciex Qtrap (ESIMS) and HRESIMS was accomplished on a Waters Synapt GII. PDA-LC/MS analysis was performed using a Waters Alliance 2965 HPLC system, attached to a Waters 2996 PDA detector, with a Waters Xterra C_{18}-column (5 μm, 2.1 mm i.d. × 150 mm) that was connected to an AB Sciex Qtrap MS/MS system equipped with an ESI probe. Middle-pressure liquid chromatography was accomplished using a Teledyne ISCO CombiFlash Companion. Preparative HPLC was performed using a Waters 600E pump system with Senshu Pak Pegasil ODS column (5 μm, 20 mm i.d. × 250 mm).

Culture condition

Streptomyces sp. RK88-1355 was cultured in a 500 ml of cylindrical flask (K1 flask) containing 70 ml of culture medium (glucose 1%, soluble starch 2%, soybean meal 1.5%, malt extract 0.5%, vegetable extract 10%, potato dextrose 2.5%, KH_2PO_4 0.05% and $MgSO_4.7H_2O$ 0.05%) for 96 h at 28 °C on a rotary shaker with agitation of 150 r.p.m. 140 ml of each preculture was used to inoculate two of 30-l jar fermentors that contained 15 l of the same culture medium, which were cultured with stirring speed at 100 r.p.m. and an aeration rate of 10 l min^{-1} for 4 days.

Construction of fraction library

The fraction library of microbial metabolites was constructed from 36.08 g of ethyl acetate extract, which was prepared from 30 l of culture broth. The methodology of fraction library construction was followed as in the previously described method.[9]

Construction of NPPlot

Each fraction was analyzed by PDA-LC/MS with an acetonitrile/0.05% formic acid aqueous gradient system (acetonitrile: 5–100% in 30 min, and hold for 15 min). The retention time of HPLC recorded on UV chromatogram and *m/z*

Table 5 ^{1}H NMR chemical shifts for compounds 1 and 2 in $CDCl_3$

	1	*2*		*1*	*2*
Position	δ_H *(m, J in Hz)*	δ_H *(m, J in Hz)*	*Position*	δ_H *(m, J in Hz)*	δ_H *(m, J in Hz)*
1			31	2.88 (3H, s)	2.89 (3H, s)
2			32	1.35 (3H, d, 6.9)	1.35 (3H, d, 7.4)
4			33-NH	8.85 (1H, br d, 9.2)	8.86 (1H, d, 8.6)
5	6.25 (1H, d, 10.6)	6.28 (1H, d, 10.5)	34		
5a	5.08 (1H, d, 10.6)	5.11 (1H, d, 10.5)	35	1.29 (1H, dd, 9.2, 5.7)	1.30 (1H, m)
5c	2.47 (3H, s)	2.88 (1H, dddd, 13.2, 7.4, 7.4, 7.4)		1.88 (1H, dd, 7.4, 5.7)	1.88 (1H, dd, 8.6, 6.0)
		3.01 (1H, dddd, 13.2, 7.4, 7.4, 7.4)	36	1.72 (1H, m)	1.69 (1H, m)
5d		1.37 (3H, t, 7.4)	37	1.13 (3H, d, 6.3)	1.14 (3H, d, 6.3)
7			38	3.39 (3H, s)	3.42 (3H, s)
8	4.86 (1H, m)	4.91 (1H, m)	39	3.03 (3H, s)	3.04 (3H, s)
9-NH	6.40 (1H, d, 8.6)	6.42 (1H, d, 8.6)	40	1.36 (3H, d, 6.9)	1.37 (3H, d, 7.4)
10			41-NH	8.85 (1H, br d, 9.2)	8.84 (1H, d, 9.4)
11	4.95 (1H, dd, 9.2, 4.1)	4.91 (1H, m)	42		
12	4.67 (1H, d, 11.4)	4.67 (1H, d, 10.6)	2′		
	4.76 (1H, dd, 11.4, 4.1)	4.76 (1H, dd, 10.6, 4.6)	3′		
14			4′	7.67 (1H, s)	7.67 (1H, s)
15			4a′		
17			5′	7.69 (1H, m)	7.70 (1H, m)
18	5.77 (1H, d, 11.4)	5.72 (1H, d, 11.1)	6′	7.48 (1H, m)	7.49 (1H, m)
18a	3.19 (1H, dd, 14.3, 11.4)	3.14 (1H, dd, 13.7, 11.1)	7′	7.47 (1H, m)	7.51 (1H, m)
	4.42 (1H, d, 14.3)	4.37 (1H, d, 13.7)	8′	7.68 (1H, m)	7.71 (1H, m)
20			8a′		
21	4.83 (1H, m)	4.82 (1H, m)	3′-OH	11.29 (1H, s)	11.30 (1H, s)
22-NH	6.49 (1H, d, 8.0)	6.47 (1H, d, 9.0)	2″		
23			3″		
24	4.90 (1H, dd, 9.2, 4.3)	4.94 (1H, dd, 9.4, 4.6)	4″	7.66 (1H, s)	7.67 (1H, s)
25	4.67 (1H, d, 11.5)	4.63 (1H, d, 10.7)	4a″		
	4.77 (1H, dd, 11.5, 4.3)	4.82 (1H, dd, 10.7, 4.6)	5″	7.69 (1H, m)	7.70 (1H, m)
27	1.25 (1H, dd, 9.7, 5.7)	1.28 (1H, m)	6″	7.48 (1H, m)	7.47 (1H, m)
	1.86 (1H, dd, 7.7, 5.7)	1.90 (1H, dd, 8.0, 5.7)	7″	7.47 (1H, m)	7.51 (1H, m)
28	1.68 (1H, m)	1.75 (1H, m)	8″	7.68 (1H, m)	7.71 (1H, m)
29	1.05 (3H, d, 6.3)	1.06 (3H, d, 6.3)	8a″		
30	3.38 (3H, s)	3.41 (3H, s)	3″-OH	11.29 (1H, s)	11.30 (1H, s)

^{1}H NMR at 500 MHz was referenced to $CHCl_3$ (δ 7.24).

values of each metabolite within the fraction were used to generate a spectral database, namely NPPlot. In NPPlot, each metabolite was plotted on a 2D area by retention time of HPLC on x axis and m/z values on y axis.[9]

Isolation of 1–3

The 33rd fraction of the third middle-pressure liquid chromatography fraction was purified by C_{18}-HPLC at flow rate of 9 ml min^{-1} with acetonitrile/water (50:50) under isocratic elution to afford compounds **1** (8.8 mg) and **2** (1.5 mg) as pale yellow amorphous solids. The 37th fraction of the seventh middle-pressure liquid chromatography fraction was applied to the same C_{18}-HPLC system and eluted with acetonitrile/water (70:30) in isocratic fashion to yield 5.7 mg of compound **3**. The physicochemical properties of compounds **1** and **2** were summarized in Table 1. ^{1}H and ^{13}C NMR chemical shifts of **1** and **2** in chloroform-*d* were summarized in Tables 2 and 5. For compound **3**, it was found to be identical with UK-63,598.[20] The physicochemical properties of compound **3** were as followed: yellow amorphous solid; $[\alpha]_{589}^{25}$ −120° (*c* 0.04, MeOH); UV (MeOH) λ_{max} (log ε) 218 (4.79), 231 (4.79), 299 (4.00), 357 (3.96); IR ν_{max} (ATR) cm^{-1} 3370, 2930, 1735, 1655, 1510; ESIMS m/z 1127 $[M+H]^+$; HRESIMS found m/z 1127.3949 $[M+H]^+$ calcd for $C_{53}H_{63}N_{10}O_{14}S_2$ 1127.3967; ^{13}C NMR, δ_C: 11.8 (C-37), 11.9 (C-29), 15.3 (C-5c), 16.7 (C-40), 18.0 (C-32), 24.6 (C-36), 25.1 (C-28), 26.0 (C-27), 26.2 (C-18a and C-35, 2C), 29.8 (C-39), 31.8 (C-31), 35.9 (C-30), 36.6 (C-38), 45.7 (C-8), 46.2 (C-21), 47.0 (C-2), 47.1 (C-15), 50.7 (C-11), 51.4 (C-5a), 51.7 (C-24), 54.3 (C-18), 60.5 (C-5), 63.9 (C-25), 64.3 (C-12), 121.2 (C-4′), 121.3 (C-4″), 126.8 (C-5′ and C-5″, 2C), 127.7 (C-7′), 127.7 (C-7″), 128.6 (C-8′ and C-8″, 2C), 128.9 (C-6′), 129.0 (C-6″), 132.4 (4a′), 132.4 (4a″), 133.7 (2′), 133.7 (2″), 141.2 (8a′), 141.3 (8a″), 153.7 (C-3′ and C-3″, 2C), 167.3 (C-10), 167.7 (C-23), 168.5 (C-42), 168.6 (C-34), 169.3 (C-1), 169.6 (C-14), 170.4 (C-4), 171.6 (C-17), 172.9 (C-20) and 173.2 (C-7).

In vitro cytotoxicity assay

The human promyelocytic leukemia cell line HL-60[27] was cultured at 37 °C in RPMI-1640 medium (Invitrogen/Life Technologies, Carlsbad, CA, USA), supplemented with 10% fetal bovine serum (FBS; Sigma-Aldrich, St Louis, MO, USA). The human cervix epidermoid carcinoma cell line HeLa was cultured at 37 °C in Dulbecco's modified Eagle's medium (DMEM; Invitrogen/Life Technologies), supplemented with 10% FBS. tsFT210 cells,[28] the mouse temperature-sensitive cdc2 mutant cell line of the mammary carcinoma FM3A, were cultured at 32 °C in RPMI-1640 medium supplemented with 5% calf serum (CS; PAA Laboratories GmbH, Buckinghamshire, UK). *src*^{ts}-NRK cells,[19] the rat kidney cells infected with ts25, a T-class mutant of Rous sarcoma virus Prague strain, were cultured at a permissive temperature (32 °C) in Minimum Essential Medium (MEM; Sigma-Aldrich) supplemented with 10% CS. Each cell line was seeded into a 96-well plate (1.5×10^4 cells per well for HL-60, 4×10^3 cells per well for HeLa, 1.6×10^4 cells per well for tsFT210 and 1.0×10^4 cells per well for *src*^{ts}-NRK) and then exposed to test compounds for 48 h. Following 48-h exposures to test compounds, cell proliferation was determined using a Cell Count Reagent SF (Nacalai Tesque, Kyoto, Japan) according to the manufacturer's instructions. Briefly, following a 48-h exposure, a 1/10 volume of WST-8 solution was added to each well, and the plates were incubated at 37 °C for 1 h. Then, cell growth was measured as the absorbance at 450 nm on a microplate reader (Perkin Elmer).

Antimicrobial activity assay

In broth microdilution assay, *S. aureus* 209, *E. coli* HO141, *C. albicans* JCM1542, *A. fumigatus* Af293, and *M. oryzae* kita-1 were used as test strains. For *S. aureus* and *E. coli*, 100 µl of cell suspension containing 1% of precultured broth was plated into a 96-well plate. Test compounds were added to the culture medium, and the plates were incubated at 37 °C for 24 h. For *C. albicans* and *A. fumigatus*, 200 µl of inoculum suspension containing 0.1% of a 0.5 McFarland standard suspension was plated into a 96-well plate. Test compounds were added to the culture medium, and the plates were incubated at 28 °C for 24 h (*C. albicans*) and 48 h (*A. fumigatus*). For *M. oryzae*, 200 µl of cell suspension containing 2% of precultured broth was plated into a 96-well plate. After added with test compounds, the plates were incubated at 28 °C for 48 h. The growths of these microorganisms were measured by absorbance at 600 nm.

ACKNOWLEDGEMENTS

We are grateful to Drs Y Futamura, H Hayase, and MS H Aono in RIKEN for biological activity assay. We also thanked Mr A Subedi in RIKEN for helpful assistance. The USM Fellowship and RIKEN IPA program were acknowledged for providing financial support in this research to CL Lim. This work was supported in part by a Grant-in-Aid for Scientific Research (A) from the Ministry of Education, Culture, Sports and Technology of Japan, the Program for Promotion of Basic and Applied Researches for Innovations in Bio-oriented Industry and Health, and Labour Sciences Research Grant.

1 Mollinari, G. Natural products in drug discovery: present status and perspectives. *Adv. Exp. Med. Biol.* **655,** 13–27 (2009).
2 Larsson, J., Gottfries, J., Muresan, S. & Backlund, A. ChemGPS-NP: tuned for navigation in biologically relevant chemical space. *J. Nat. Prod.* **70,** 789–794 (2007).
3 Mishra, B. B. & Tiwari, V. K. Natural products: an evolving role in future drug discovery. *Eur. J. Med. Chem.* **46,** 4769–4807 (2011).
4 Osada, H. An overview on the diversity of actinomycete metabolites. *Actinomycetol.* **15,** 11–14 (2001).
5 Newman, D. J. & Cragg, G. M. Natural products as sources of new drugs over the 30 years from 1981 to 2010. *J. Nat. Prod.* **75,** 311–335 (2012).
6 Dobson, C. M. Chemical space and biology. *Nature* **432,** 824–828 (2004).
7 Osada, H. Bioprobes for investigating mammalian cell cycle control. *J. Antibiot.* **51,** 973–982 (1998).
8 Osada, H. in *Protein targeting with small molecules: Chemical biology techniques and applications* (ed. Osada, H.) (Wiley, New Jersey 1–10, 2009).
9 Osada, H. & Nogawa, T. Systematic isolation of microbial metabolites for natural products depository (NPDepo). *Pure Appl. Chem.* **84,** 1407–1420 (2011).
10 Nogawa, T. *et al.* Verticilactam, a new macrolactam isolated from a microbial metabolite fraction library. *Org. Lett.* **12,** 4564–4567 (2010).
11 Cheng, X. *et al.* A new antibiotic, tautomycin. *J. Antibiot.* **40,** 907–909 (1987).
12 Magae, J., Watanabe, C., Osada, H., Cheng, X. C. & Isono, K. Induction of morphological change of human myeloid leukemia and activation of protein kinase C by a novel antibiotic, tautomycin. *J. Antibiot.* **41,** 932–937 (1988).
13 Cheng, X. C., Ubukata, M. & Isono, K. The structure of tautomycin, a dialkylmaleic anhydride antibiotic. *J. Antibiot.* **43,** 809–819 (1990).
14 Nogawa, T. *et al.* Spirotoamides A and B, novel 6,6-spiroacetal polyketides isolated from a microbial metabolite fraction library. *J. Antibiot.* **65,** 123–128 (2012).
15 Cheng, X. C. *et al.* A new antibiotic, tautomycetin. *J. Antibiot.* **42,** 141–144 (1989).
16 Cheng, X. C., Ubukata, M. & Isono, K. The structure of tautomycetin, a dialkylmaleic anhydride antibiotic. *J. Antibiot.* **43,** 890–896 (1990).
17 Panthee, S. *et al.* Furaquinocins I and J: novel polyketide isoprenoid hybrid compounds from *Streptomyces reveromyceticus* SN-593. *J. Antibiot.* **64,** 509–513 (2011).
18 Takahashi, S. *et al.* Biochemical characterization of a novel indole prenyltransferase from *Streptomyces* sp. SN-593. *J. Bacteriol.* **192,** 2839–2851 (2010).
19 Osada, H., Koshino, H., Isono, K., Takahashi, H. & Kawanishi, G. Reveromycin A, a new antibiotic which inhibits the mitogenic activity of epidermal growth factor. *J. Antibiot.* **44,** 259–261 (1991).
20 Rance, M. J. *et al.* UK-63,052 complex, new quinomycin antibiotics from *Streptomyces braegensis* subsp. *Japonicus*; Taxonomy, fermentation, isolation, characterization and antimicrobial activity. *J. Antibiot.* **42,** 206–217 (1989).
21 Takahashi, K. *et al.* SW-163C and E, novel antitumor depsipeptides produced by *Streptomyces* sp. II. Structure elucidation. *J. Antibiot.* **54,** 622–627 (2001).
22 Boger, D. L. & Ichikawa, S. Total syntheses of thiocoraline and BE-22179: Establishment of relative and absolute stereochemistry. *J. Am. Chem. Soc.* **122,** 2956–2957 (2000).
23 Baz, J. P., Canedo, L. M., Fernandez Puentes, J. L. & Silva Elipe, M. V. Thiocoraline, a novel depsipeptide with antitumor activity produced by a marine *Micromonospora*. II. Physico-chemical properties and structure determination. *J. Antibiot.* **50,** 738–741 (1997).
24 Socha, A. M., LaPlante, K. L., Russell, D. J. & Rowley, D. C. Structure-activity studies of echinomycin antibiotics against drug-resistant and biofilm-forming *Staphylococcus aureus* and *Enterococcus faecalis*. *Bioorg. Med. Chem. Lett.* **19,** 1504–1507 (2009).
25 Ko, J., Chin, S., Kyo, T., Mizogami, K. & Hanada, K. Japan Patent. 06316595 (1994).
26 Park, Y. S., Kim, Y. H., Kim, S. K. & Choi, S. J. A new antitumor agent: methyl sulfonium perchlorate of echinomycin. *Bioorg. Med. Chem. Lett.* **8,** 731–734 (1998).
27 Osada, H., Magae, J., Watanabe, C. & Isono, K. Rapid screening method for inhibitors of protein kinase C. *J. Antibiot.* **41,** 925–932 (1988).
28 Osada, H., Cui, C. B., Onose, R. & Hanaoka, F. Screening of cell cycle inhibitors from microbial metabolites by a bioassay using a mouse cdc2 mutant line, tsFT210. *Bioorg. Med. Chem.* **5,** 193–203 (1997).

Supplementary Information accompanies the paper on The Journal of Antibiotics website (http://www.nature.com/ja)